Heavy-ion optical potential for sub-barrier fusion deduced from a dispersion relation

B. T. Kim and H. C. Kim
Department of Physics, Sung Kyun Kwan University, Suwon 170, Korea

K. E. Park
Department of Physics Education, Cheju National University, Cheju 590, Korea
(Received 23 September 1987)

The heavy-ion energy-dependent optical potentials for the $^{16}O+^{208}Pb$ system are deduced from a dispersion relation. These potentials are used to analyze the elastic scattering, fusion, and spin distributions of compound nuclei for the system in a unified way based on the direct reaction theory. It turns out that the energy dependence of the optical potential is essential in explaining the data at near- and sub-barrier energies. The real part of the energy-dependent optical potential deduced was also used in calculating the elastic and fusion cross sections by the conventional barrier penetration model using an incoming wave boundary condition. The predictions of the elastic scattering, fusion cross sections, and the spin distributions of compound nuclei are not satisfactory compared with those from the direct reaction approach. It seems to originate from the fact that this model neglects absorption around the Coulomb barrier region.

I. INTRODUCTION

The sub-barrier fusion reactions of two heavy ions have attracted much interest recently. The observed fusion yields are much larger than those predicted by the conventional barrier penetration model (BPM).[1,2] Several approaches have been suggested to interpret this anomalous behavior.

One method is based on the BPM and considers couplings to nonelastic channels,[3-6] some of which allow for lowering an effective potential barrier (sum of nuclear, Coulomb, and centrifugal potentials) resulting in enhanced fusion. The Nagarajan and Stachler group[7-10] pointed out that these effects can be put into the simple BPM if the potential used is deduced from a dispersion relation. Since absorption decreases rapidly as the energy decreases towards the Coulomb barrier, the corresponding polarization as a function of energy has a peak around the top of the barrier. Thus the real part of the potential including the polarization also depends upon the incident energy, and the effective potential barrier is lowered at near-barrier energies. In order to calculate the penetrability through the barrier, the incoming wave boundary condition[4,5] or a short-ranged imaginary potential[6,9,10] was used in the BPM so that fusion does not occur until the barrier has been traversed.

Another approach is founded on the direct reaction theory, in which fusion is considered to proceed through the formation of a compound nucleus.[11,12] Absorption into fusion channels is assumed to be due to the inner portion of the imaginary part W of the usual optical potential, the outer portion being responsible for the direct reactions. In other words, a fusion potential W_F is defined as the inner part of W, i.e., the part with $r < R_F$, R_F being called the fusion radius. Such an idea was quite successful[12] in explaining the experimental fusion cross sections of a large number of sets of two heavy-ion partners.

Whether these models can reproduce the fusion data largely depends on the choice of a potential. Of course the potential should also reproduce the elastic scattering, other direct reaction phenomena, and the features of fusion such as spin distributions of compound nucleus formation.[13] Unfortunately, it is difficult to find a potential which reproduces all these data at the same time. The calculated spin distributions in the BPM with potentials deduced from a dispersion relation are generally smaller than the observed ones and the potentials which explain the fusion data are to be readjusted to fit the elastic scattering.[9,14] The direct reaction approach usually employs energy-independent optical potentials because of a lack of information on the energy-dependence of the optical potentials for most systems.

The experimental and theoretical works on the energy dependence of the optical potentials have been recently reported for some systems,[15,16] In this paper, we present analysis of elastic scattering, fusion, and spin distributions of the $^{16}O + ^{208}Pb$ system[17-20] in a unified way within the direct reaction theory by using an energy-dependent optical potential deduced from a dispersion relation. Similar analyses are done by using the incoming wave boundary condition and a comparison of the different results is made.

II. OPTICAL POTENTIAL DEDUCED FROM A DISPERSION RELATION

The elastic scattering data recently accumulated show[8,15,16] that the imaginary part of the optical potential diminishes quite rapidly as the incident energy becomes lower than the Coulomb barrier. This can be understood from the fact that fewer reaction channels are

open when the beam energy is lower. When the energy-dependent optical potential at a fixed radius around the strong absorption radius is plotted as a function of energy, the real part is shown to be a bell shape, peaked around the Coulomb barrier. This is because the coupling of the elastic channel to other reaction channels gives rise to the polarization effects. These phenomena can be explained by the dispersion relation between the real and imaginary parts of the optical potential.[7,8] The sudden increase in the real part of the potential at near-barrier energies allows for lowering the barrier and enhances the penetrability of the incident waves through the barrier. It can account for anomalously large fusion cross sections recently observed in sub-barrier heavy-ion fusion reactions. Therefore, near the barrier, the energy dependence of the optical potential could be crucial in explaining not only the elastic scattering but also fusion.

We now generate a local, energy-dependent optical potential based on the dispersion relation. The real potential can be obtained from a dispersion relation[7,8] as

$$V(r,E)=V(r,E_s)+\frac{E-E_s}{\pi}P\int_0^\infty \frac{W(r,E')dE'}{(E'-E_s)(E'-E)}\ , \tag{1}$$

where P denotes the principal value. The first term on the right hand side, $V(r,E_s)$ is the bare potential and the second one the polarization potential due to couplings. The bare potential is chosen to be of Woods-Saxon type and E_s in the bare potential is the energy where the normalization is done to give a correct magnitude of the depth parameter, V_0 of the Woods-Saxon potential.

We assume a factorization of the imaginary potential into the radial and energy parts as

$$W(r,E)=W_r(r)\times W_e(E) \tag{2}$$

and further assume $W_r(r)$ to be of the Woods-Saxon form,

$$W_r(r)=\frac{-W_0}{1+\exp\dfrac{r-R_0}{a_0}} \tag{3}$$

and

$$W_e(E)=\frac{1}{1+\exp\dfrac{E_b-E}{a_e}}\ , \tag{4}$$

where E_b is the energy of the Coulomb barrier and a_e the diffuseness parameter of the energy dependence.

The radial dependence of the bare and imaginary potential is assumed to have the same geometry. It means that at a given energy, the radial dependence of both real and imaginary potential is again of a Woods-Saxon type and the potential depth depends only on the incident energy. We also performed calculations with potentials with a constant depth parameter and energy-dependent radius parameters. We did not obtain any significant differences in the results between the two methods.

III. ANALYSIS OF THE $^{16}O+^{208}Pb$ SYSTEM

A lot of experimental data of the elastic scattering and fusion reaction for the $^{16}O + ^{208}Pb$ system in a wide range of the incident energy have been accumulated.[17–20] In Fig. 1, the real and imaginary potential strengths at $R=12.4$ fm deduced from the optical model analysis of the observed elastic scattering are plotted. It is clearly seen that the imaginary part becomes weaker as the incident energy approaches the Coulomb barrier, while the real part increases rapidly. It thus implies the existence of the dispersion relation between the real and imaginary parts of the optical potential.

We generate the real and imaginary parts of the optical potential for the $^{16}O + ^{208}Pb$ system by a method discussed in Sec. II. The Coulomb barrier energy parameter E_b and the energy diffuseness parameter a_e were chosen[7] to be 80 and 6 MeV, respectively. The normalization of the potential was taken at $E_s=102$ MeV. The potential parameters for the radial dependence are $V_0=110$ MeV, $W_0=70$ MeV, $a_0=0.50$ fm, and $r_0=1.23$ fm. r_0 is related to R_0 by $R_0=r_0(A_1^{1/3}+A_2^{1/3})$ where A_1 and A_2 are mass numbers of the colliding partners. The solid curves in Fig. 1 are the results of calculations evaluated at $R=12.4$ fm. These parameters reproduce well both the real and imaginary parts.

We also generated potentials by using the parameters suggested by Mahaux *et al.*[8] Because of the smaller a_e value chosen (4.55 MeV instead of our value of 6 MeV), $V(R=12.4$ fm,$E)$ has a sharper peak around $E_{\rm lab}=80$ MeV. Otherwise they looked the same, and the calculated results of elastic scattering and fusion cross sections did not show many differences. Throughout this paper, we present the results with potentials shown in Fig. 1.

A. Direct reaction approach

Recently, Udagawa, Kim, and Tamura[11,12] proposed a fusion model based on the direct reaction approach.

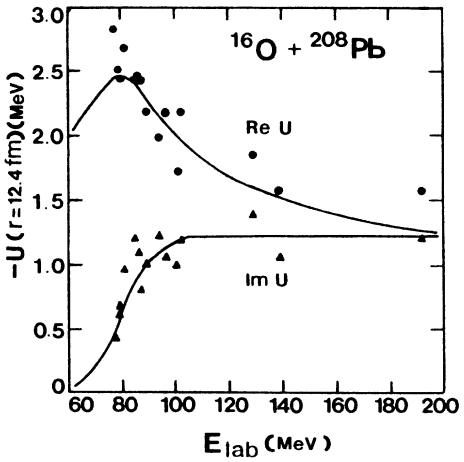

FIG. 1. The real and imaginary strengths evaluated at $R=12.4$ fm of the optical potential as a function of the bombarding energy for the $^{16}O + ^{208}Pb$ system. The solid curves represent a calculated dispersion relation. The data are employed from Ref. 15.

Their basic idea is that the imaginary part of the optical potential can be dissected into two parts; one of them, $W_F(r)$, is responsible for fusion and the other, $W_D(r)$, accounts for the direct reactions. Then the fusion cross section is expressed as

$$\sigma_F = \frac{\pi}{k^2} \sum_l (2l+1) T_{F;l} \ . \tag{5}$$

The transmission coefficients $T_{F;l}$ in Eq. (5) can be written as

$$T_{F;l} = \frac{8}{\hbar v} \int_0^\infty |\chi_l(r)|^2 W_F(r) dr \ , \tag{6}$$

where v is the relative velocity. The $\chi_l(r)$ is the partial scattering wave function calculated with the full optical potential, $U = V + iW$, as a solution of

$$-\frac{\hbar^2}{2\mu}\frac{d^2\chi_l(r)}{dr^2} + \left[U(r) + \frac{l(l+1)\hbar^2}{2\mu r^2} \right] \chi_l(r) = E\chi_l(r) \ . \tag{7}$$

For simplicity, they introduced a fusion potential W_F defined as the inner part of W,

$$W_F = \begin{cases} W, & r < R_F \\ 0, & r \geq R_F \end{cases} \tag{8}$$

and treated R_F as a parameter to be determined by fitting the calculated fusion cross sections to the experimental data.

Our energy-dependent optical potentials generated from a dispersion relation are plugged into Eq. (7) to calculate χ_l. The phase shifts of χ_l give us the elastic scattering cross sections, since the full optical potential is used in Eq. (7). We present the results of calculated differential elastic scattering cross sections at $E_{\rm lab} = 80$, 90, and 102 MeV as solid curves in Fig. 2. It can be seen that the solid curves fit the experimental data well, which means that our energy-dependent potentials seem to be a good choice as far as the elastic scattering is concerned.

The transmission coefficients of Eq. (6) are then calculated by choosing $r_F = 1.44$ fm. The calculated fusion cross sections as a function of the incident beam energy are displayed as a solid curve in Fig. 3. The fits to the fusion data in the energy range considered here are very good, except at very low energies. The imaginary part used in this region seems to be still too large. Unfortunately there is not much information of the elastic scattering below $E_{\rm lab} = 80$ MeV, and the dispersion relation between the real and imaginary parts is not clearly settled at these very low energies yet.

Spin distributions of compound nuclei formed by heavy-ion fusion reactions became recently available[21–24] and provided an opportunity for more stringent tests of our understanding of the fusion reaction mechanism. The direct reaction approach for fusion has indeed been successful in reproducing the measured spin distributions for some systems.[13] We calculated mean square spin values for the $^{16}O + {}^{208}Pb$ system by using our optical potentials, and compared them with the data.[19,20,24] The

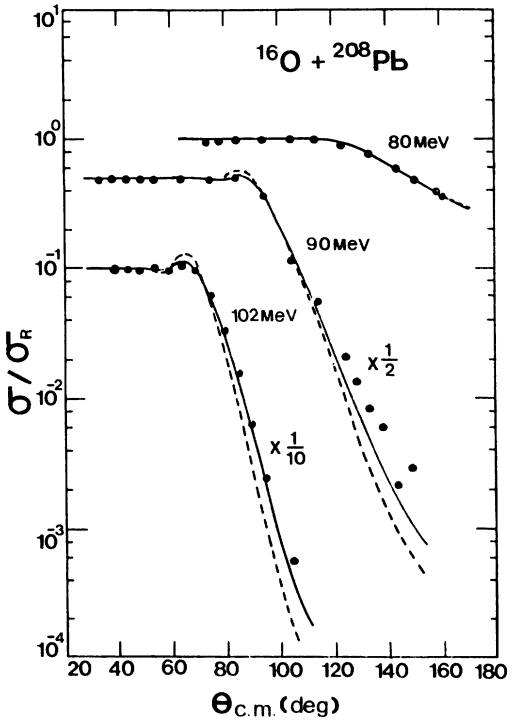

FIG. 2. The elastic scatterings of the $^{16}O + {}^{208}Pb$ system at $E_{\rm lab} = 80$, 90, and 102 MeV. The solid and dashed curves are the differential elastic scattering cross sections calculated with energy-dependent and energy-independent optical potentials, respectively. The data are taken from Ref. 17.

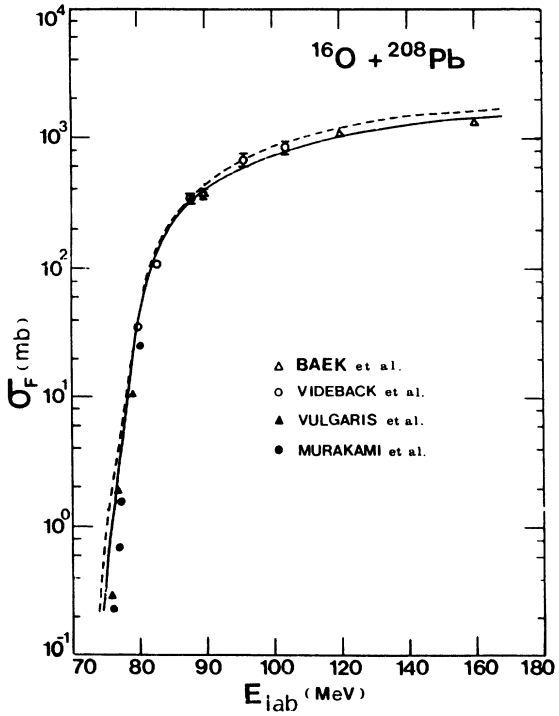

FIG. 3. The fusion excitation function of the $^{16}O + {}^{208}Pb$ system. The solid and dashed curves are the fusion cross sections calculated with energy-dependent and energy-independent optical potentials, respectively. The data are taken from Refs. 17–20.

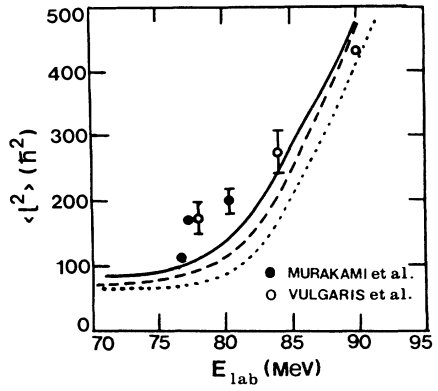

FIG. 4. Mean square spin values as a function of the bombarding energy for the $^{16}O + ^{208}Pb$ system. The solid and dashed curves are based on the direct reaction approach and the BPM with the incoming wave boundary conditions, respectively. The dotted curve represents the BPM results with renormalized potentials of $N = 0.675$.

solid curve in Fig. 4 shows the results of the calculations. Again our model reproduces the data well, although it still underestimates at around the Coulomb barrier energies.

We also made a calculation with an energy independent optical potential. The potential chosen was from the elastic scattering analysis at $E_{lab} = 80$ MeV.[17] The dashed curves in Fig. 2 represent the differential elastic scattering cross sections at $E_{lab} = 80$, 90, and 102 MeV. It is immediately seen that the fits become poorer as the energy increases, and the energy dependence of the optical potential is shown to be essential. The dashed curve in Fig. 3 shows the calculated fusion cross sections with this potential It overestimates the data, as well as the cross sections with energy-dependent potentials in both the above- and sub-barrier region.

B. BPM with the incoming wave boundary condition

As one way of calculating the transmission coefficient of Eq. (5) quantum mechanically, the BPM uses the incoming wave boundary condition.[4,5] It consists of defining a boundary radius in an effective potential pocket and assuming that only the incoming waves exist inside the boundary radius. The waves which penetrate the barrier and pass this boundary radius are all transmitted and never reflected, and thus contribute to fusion. This boundary condition gives us the transmission and reflection coefficients and, in turn, the fusion and elastic

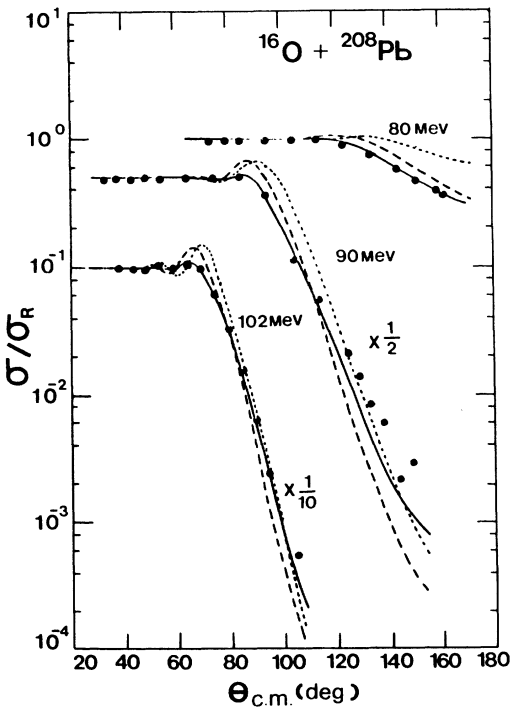

FIG. 5. Same as Fig. 2, but a comparison of results from the direct reaction approach (solid curves) with those from the BPM with an incoming wave boundary condition (dashed curves) is made. The dotted curves show the BPM results with renormalized potentials of $N = 0.675$.

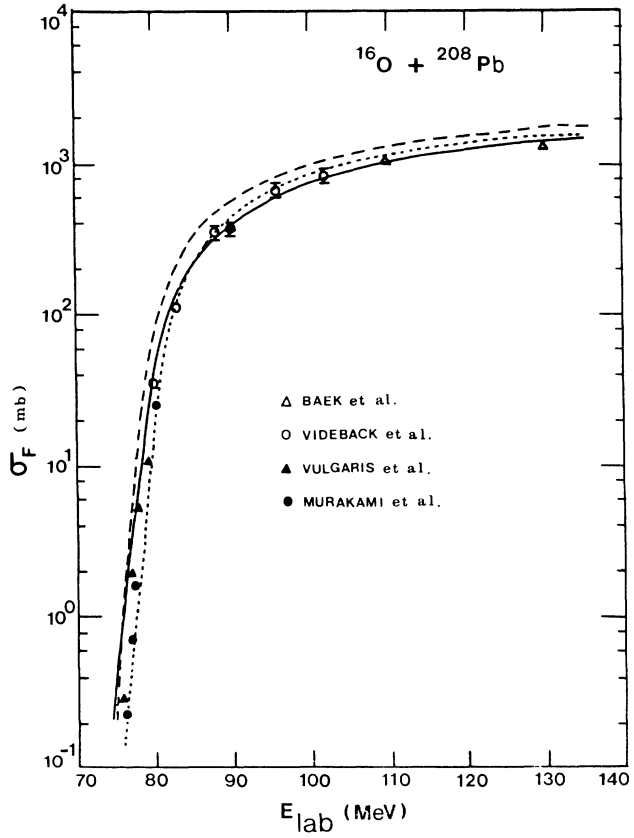

FIG. 6. Same as Fig. 3, but a comparison of results from the direct reaction approach (solid curve) with those from the BPM with an incoming wave boundary condition (dashed curve) is made. The dotted curve shows the BPM results with renormalized potentials of $N = 0.675$.

scattering cross sections.[14,25]

It is worth noting that the potential used is purely real and all the flux penetrated contribute to fusion. There is no room to consider the direct reactions other than the elastic scattering in this method unless coupled-channels calculations are done. However, very recently Nagarajan and Satchler[9] reported that the BPM can be justified, if the energy dependent potentials deduced from a dispersion relation are used, i.e., couplings to nonelastic channels are taken into account. Nevertheless, a simple renormalization procedure in determining the potential strength was still needed to reproduce the measured fusion cross sections, and spin distributions were not well reproduced.

We now present the results of calculations by imposing the incoming wave boundary condition, in the framework of the BPM, and by employing the real potentials deduced from a dispersion relation discussed previously. The calculations were performed following Park *et al.*[14,25] The results of elastic scattering and fusion cross sections are displayed as dashed curves in Figs. 5 and 6, respectively, and are compared with those obtained from the direct reaction approach as solid curves. Neither the elastic scattering data nor the fusion cross sections are well reproduced. Because of a lack of absorption due to direct reaction channels in the grazing region, the elastic cross sections near the grazing angle are greatly overestimated. At the backward angles, the absorption caused by only imposing the incoming wave boundary condition could not account for the data either.

The calculated fusion cross sections overestimate the data in the whole energy region considered here. It implies that the real potentials are quite deep and thus make the Coulomb barrier lower, resulting in large fusion cross sections. We simply renormalized the well depth of the real potential so that the fusion data can be reproduced. The dotted curve in Fig. 6 represents such results with a normalization factor of $N=0.675$. As far as the fits to the fusion data are concerned, the results are very good. However, the fits to the elastic scattering become poorer than those without normalization as seen in Fig. 5.

Spin distributions are also calculated with and without normalization, and displayed as dotted and dashed curves, respectively, in Fig. 4. Both of them underestimate the observed spin distributions.

IV. CONCLUSION

We deduced heavy-ion optical potentials for the $^{16}O + ^{208}Pb$ system from a dispersion relation. These local, energy-dependent optical potentials are employed to analyze the measured differential elastic cross sections, fusion excitation functions, and spin distributions of compound nuclei on one footing of the direct reaction theory. All three reaction phenomena are well reproduced at the same time.

The real part of the optical potential is also substituted into the conventional barrier penetration model with an incoming wave boundary condition. This method predicts spin distributions poorly and the potentials, which are renormalized in order to fit the observed fusion cross sections, fail to explain the elastic scattering data.

Instead of imposing an incoming wave boundary condition, the use of the short-ranged imaginary optical potential has been suggested.[6,9,10] They obtained very similar results to those obtained with an incoming wave boundary condition here. What they claim is that no imaginary potential in the surface region is necessary as long as the polarization effects, which arise from the coupling of the elastic channel to all nonelastic channels, are correctly taken into account in the one-channel calculations, i.e., the potentials deduced from a dispersion relation are used. Our analyses, which use the energy-dependent optical potential based on a dispersion relation, show that this simple argument is not valid, and absorption must take place in the surface region in order to explain the elastic scattering, fusion, and spin distributions at the same time. Whether the range of the imaginary part, which is solely responsible for fusion, is short, say $r_0 \approx 1.0$ fm, as claimed in the BPM or long, say $r_0 \approx 1.4$ fm, is a current issue in understanding the fusion mechanism. Currently, Hong *et al.*[26] are investigating this issue in a phenomenological way.

ACKNOWLEDGMENTS

We are grateful to Dr. S.-W. Hong for his careful reading of the manuscript and to Prof. T. Udagawa for useful discussions. This work was supported by the Ministry of Education, Korea, the Basic Science Research Institute Program, 1987.

[1]L. C. Vaz, J. M. Alexander, and G. R. Satchler, Phys. Rep. **C69**, 820 (1978).
[2]J. R. Birkelund and J. R. Huizenga, Annu. Rev. Nucl. Part. Sci. **33**, 265 (1983).
[3]H. Esbensen, Nucl. Phys. **A352**, 147 (1981).
[4]C. H. Dasso, S. Landowne, and A. Winther, Nucl. Phys. **A405**, 381 (1983).
[5]R. A. Broglia, C. H. Dasso, S. Landowne, and A. Winther, Phys. Rev. C **27**, 2433 (1983).
[6]M. J. Rhodes-Brown and M. Prakash, Phys. Rev. Lett. **53**, 333 (1984).
[7]M. A. Nagarajan, C. C. Mahaux, and G. R. Satchler, Phys. Rev. Lett. **54**, 1136 (1985).
[8]C. C. Mahaux, H. Ngo, and G. R. Satchler, Nucl. Phys. **A449**, 354 (1986).
[9]M. A. Nagarajan and G. R. Satchler, Phys. Lett. B **173**, 29 (1986).
[10]G. R. Satchler, M. A. Nagarajan, J. S. Lilley, and I. J. Thompson (unpublished).
[11]T. Udagawa and T. Tamura, Phys. Rev. C **29**, 1922 (1984).
[12]T. Udagawa, B. T. Kim, and T. Tamura, Phys. Rev. C **32**, 124 (1985).
[13]B. T. Kim, T. Udagawa, and T. Tamura, Phys. Rev. C **33**, 370 (1986).
[14]K. E. Park, W. K. Lie, and B. T. Kim, New Physics (Seoul) **26**, 429 (1986).

[15]J. S. Lilley, B. R. Fulton, M. A. Nagarajan, I. J. Thompson, and D. W. Banes, Phys. Lett. **151B**, 181 (1985).
[16]B. R. Fulton, D. W. Banes, J. S. Lilley, M. A. Nagarajan, and I. J. Thompson, Phys. Lett. **162B**, 55 (1985).
[17]F. Videbaek, R. B. Goldstein, L. Grodzins, S. G. Steadman, T. A. Belote, and J. D. Garrett, Phys. Rev. C **15**, 954 (1977).
[18]B. B. Back, R. R. Betts, J. E. Gindler, B. D. Wilkins, S. Saini, M. B. Tsang, C. K. Gelbke, W. G. Lynch, M. A. McMahan, and P. A. Baisden, Phys. Rev. C **32**, 195 (1985).
[19]E. Vulgaris, L. Grodzins, S. G. Steadman, and R. Ledoux, Phys. Rev. C **33**, 2017 (1986).
[20]T. Murakami, C. C. Sahm, R. Vandenbosch, D. D. Leach, A. Ray, and M. J. Murphy, Phys. Rev. C **34**, 1353 (1986).
[21]R. Vandenbosch, B. B. Back, S. Gil, A. Lazzarini, and A. Ray, Phys. Rev. C **28**, 1161 (1983).
[22]B. Hass *et al.*, Phys. Rev. Lett. **54**, 398 (1985).
[23]P. J. Nolan, D. J. G. Love, A. Kirwan, D. J. Unwin, A. H. Nelson, P. J. Twin, and J. D. Garrett, Phys. Rev. Lett. **54**, 2211 (1985).
[24]R. Vandenbosch, T. Murakami, C. C. Sahm, D. D. Leach, A. Ray, and M. J. Murphy, Phys. Rev. Lett. **56**, 1234 (1986).
[25]W. K. Lie, K. E. Park, and B. T. Kim, Sung Kyun Rep. **37**, 113 (1986).
[26]S. W. Hong, T. Udagawa, and T. Tamura (unpublished).